[23] J. D. Thompson, D. G. Higgins, T. J. Gibson, *Nucleic Acids Res.* **1994**, *22*, 4673 – 4680.
[24] F. Jeanmougin, J. D. Thompson, M. Gouy, D. G. Higgins, T. J. Gibson, *Trends Biochem. Sci.* **1998**, *23*, 403 – 405.
[25] D. A. Berthold, M. E. Andersson, P. Nordlund, *Biochem. Biophys. Acta* **2000**, *1460*, 241 – 254.
[26] N. Guex, M. C. Peitsch, *Electrophoresis* **1997**, *18*, 2714 – 2723.
[27] *WebLab ViewerLite*, Molecular Simulations, Inc., Princeton, **1998**.

Received: December 7, 2000
Revised version: April 4, 2001 [Z 163]

Visualization of Annexin I Binding to Calcium-Induced Phosphatidylserine Domains

Andreas Janshoff,[b] Michaela Ross,[b] Volker Gerke,[c] and Claudia Steinem*[a]

KEYWORDS:

annexins · mass spectrometry · membrane proteins · phospholipids · scanning probe microscopy

Annexins are a family of structurally related eukaryotic proteins that reversibly bind membranes containing anionic phospholipids in a calcium-dependent manner.[1] More than 160 different isoforms have been found in many organisms ranging from mammals to molds.[2] The protein family is defined by its characteristic structure comprising a conserved core made up of four or eight domains of a 70-amino-acid sequence forming five α helices and a variable N-terminal region varying in length and amino acid sequence. The core domains harbor multiple calcium-binding sites, which are all located on the convex side of the molecule.[3] X-ray crystallographic analyses[4–8] and mutagenesis studies[9–13] have shown that the convex site is responsible for initial membrane binding. Calcium ions bound to these sites act as bridges connecting the protein with anionic lipid headgroups. The N-terminal region is thought to be involved in the regulation of different functions of annexins. Although exact physiological functions of annexins have not been identified yet, it has been shown that they participate in a variety of in vitro activities. In particular, some annexins such as annexins I, II, IV and VII can promote membrane aggregation and may thus be involved in cellular endo- and exocytotic pathways. It was shown that annexin I, the protein of interest in our study, is capable of aggregating and even fusing membrane vesicles.[14–16] However, the mechanism of membrane aggregation is still discussed controversially. One model postulates that membrane-bound annexin I molecules form axial dimers prior to interacting with a second membrane, while another model hypothesizes that monomeric bound annexin I interacts with the second membrane.

We utilized scanning force microscopy (SFM) on solid-supported Langmuir – Blodgett (LB) bilayers composed of 1,2-dipalmitoyl-*sn*-glycero-3-phosphocholine (DPPC) and 1,2-dipalmitoyl-*sn*-glycero-3-phosphoserine (DPPS) immobilized on mica (serving as an atomically flat substrate) to directly visualize annexin I binding with high lateral and vertical resolution, thus enabling us to distinguish between the two different models. With this technique height differences in the ångström region as well as morphological changes of the membrane structure and domain formation can be observed in a physiological environment.

Topographic images of an LB bilayer composed of DPPC as the first leaflet and DPPC/DPPS (4:1) representing the uppermost layer pointing to the aqueous phase are mostly featureless, with some defects occurring as dark spots in the SFM images. Addition of a 1 μM annexin I solution in 50 mM Tris (pH 7.4), 1 mM $CaCl_2$ to the bilayer results in the appearance of circular domains with sizes of 3 – 10 μm (Figures 1a and b) that are attributed to specifically adsorbed annexin I. These protein domains occupy (35 ± 3) % of the overall area, exhibit an average height of (3.2 ± 0.3) nm as obtained from a height analysis (Figure 1c), and are stable in a calcium-containing buffer for several hours. The thickness of the annexin layer compares well with the molecular dimension of annexin I as determined by X-ray crystallography, indicating that the protein binds in a monomeric fashion.[4, 17] Recently, Bitto et al., employing X-ray specular reflectivity measurements, also found that annexin I binds as a monomer or monolayer to 1-palmitoyl-2-oleoyl-*sn*-glycero-3-phosphoserine (POPS)/1-palmitoyl-2-oleoyl-*sn*-glycero-3-phosphoethanolamine (POPE)/1-palmitoly-2-oleoyl-*sn*-glycero-3-phosphocholine (POPC) (2:5:2) monolayers at the air – water interface. They determined a protein thickness of (3.1 ± 0.2) nm.[18] Remarkably, lateral movement of the protein domains was not observed in the Ca^{2+}-containing buffer within three hours indicating that the lateral mobility of the lipids is low, as is expected for gel-phase lipids at room temperature. Crystallization of the protein, however, did not occur as it was reported for annexin V on a DOPC/DOPS (4:1) membrane immobilized on mica.[19, 20] In

[a] *Prof. Dr. C. Steinem*
Institut für Analytische Chemie, Chemo- und Biosensorik
Universität Regensburg
93040 Regensburg (Germany)
Fax: (+49) 941-943-4491
E-mail: claudia.steinem@chemie.uni-regensburg.de
[b] *Prof. Dr. A. Janshoff,[+] M. Ross*
Institut für Biochemie
Westfälische Wilhelms-Universität
Wilhelm-Klemm-Strasse 2, 48149 Münster (Germany)
[c] *Prof. Dr. V. Gerke*
Institut für Medizinische Biochemie
Zentrum für Molekularbiologie der Entzündung
Westfälische Wilhelms-Universität
von-Esmarch-Strasse 56, 48149 Münster (Germany)
[+] *Present address*
Institut für Physikalische Chemie
Johannes-Gutenberg-Universität
Jakob-Welder-Weg 11, 55128 Mainz (Germany)

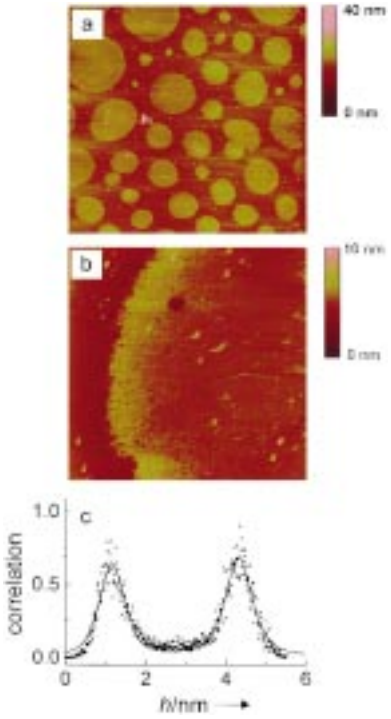

Figure 1. *a: Scanning force microscopy image (topography) of a Langmuir–Blodgett bilayer composed of DPPC as a first monolayer and a second DPPC/DPPS (4:1) monolayer deposited onto mica from a water subphase after addition of 1 μM annexin I in 50 mM Tris (pH 7.4), 1 mM $CaCl_2$. The image size is 40 × 40 μm². b: Topographic image of one domain with adsorbed annexin I. Image size: 3 × 3 μm². c: Height analysis of a topographic image of annexin I domains adsorbed onto a DPPC/DPPS lipid layer. The histogram displays a Gaussian-filtered version of a depth analysis. Two well-separated height distributions attributed to the protein and the lipid layer, respectively, are decomposed by fitting mixed Lorentzian/Gaussian functions to the data (shown as a solid line). The height difference between the two peaks is 3.2 nm.*

contrast to our experiments, Reviakine et al.[19, 21] used lipids that were in the fluid state at room temperature, resulting in a larger lateral lipid mobility on the surface. This may facilitate the crystallization process due to possible rearrangement of the protein molecules on the surface. However, it is also conceivable that the proper conditions for crystallization have not been found yet or that annexin I does not tend to form two-dimensional crystals in general. From the densely packed protein domains on the lipid bilayer it is evident that bound annexin I molecules are capable of laterally aggregating on the membrane surface. Increasing the annexin I concentration did not alter the protein domains; protein adsorption remained solely restricted to the circularly shaped domains and a larger occupancy of the surface or multilayer formation was not observed. At concentrations below 1 μM, annexin I adsorbs on the surface with submonolayer coverage and imaging in contact mode becomes cumbersome due to the high lateral force exerted on the individual proteins. However, full coverage of the DPPS-enriched domains with tightly packed annexin I reduces the lateral force on individual proteins considerably, which results in images of good quality (Figure 1).

We hypothesized that DPPS-enriched domains are formed within the LB monolayer due to the presence of calcium ions in the subphase. This was confirmed by employing time-of-flight secondary-ion mass spectrometry (TOF-SIMS) imaging of LB monolayers and lateral force microscopy of LB bilayers in aqueous solution. TOF-SIMS imaging provides a means to visualize chemical and physical properties of lipid domains after transfer from the air–water interface to a solid support, with a practical lateral resolution of 1 μm.[22, 23] We utilized this technique to image the chemical composition of DPPC/DPPS monolayers transferred onto gold surfaces at a surface pressure of 30 mN m^{-1} in dependence of different subphase conditions. Figures 2a and b display a mass map of secondary ion fragments

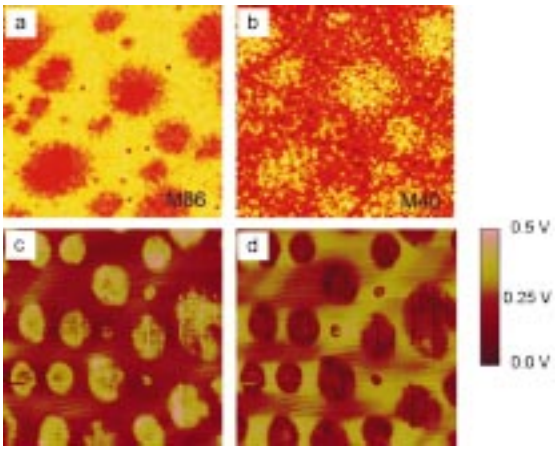

Figure 2. *a, b: Secondary-ion mass spectrometry images of positive secondary ions (SI) from a DPPC/DPPS monolayer (4:1 molar ratio) deposited at a surface pressure of 30 mN m^{-1} on gold from a water subphase. a: Positive SI ($C_5H_{12}N^+$, $M_r = 86$) specific for DPPC; b: a calcium ($M_r = 40$) map. The size of the images is 30 × 30 μm². c, d: Lateral force microscopy images of a lipid bilayer obtained in water. First, a DPPC monolayer was deposited onto mica at a surface pressure of 45 mN m^{-1} by Langmuir–Blodgett transfer followed by a second transfer of a DPPC/DPPS monolayer (4:1 molar ratio) at a surface pressure of 30 mN m^{-1}. c: forward scan; d: backward scan. The size of the images is 30 × 30 μm².*

representative of DPPC ($C_5H_{12}N^+$, $M_r = 86$) and a Ca^+ map ($M_r = 40$) of a Langmuir monolayer of DPPC/DPPS (4:1) transferred from a pure water subphase, respectively. From TOF-SIMS imaging it is evident that the circular domains, which are visible in the Ca^{2+} map due to the preferential binding of calcium ions to DPPS, are surrounded by a DPPC-enriched phase. The size of the DPPS-enriched domains is about 3–10 μm occupying an area of (35 ± 3)% consistent with the annexin I coverage observed in the SFM images. (For a more detailed TOF-SIMS analysis the reader is referred to ref. [24].) Similarly shaped domains with similar sizes were found by means of lateral force microscopy (LFM) of LB bilayers composed of DPPC and DPPC/DPPS (4:1) (Figures 2c, d). The brighter domains in the forward scan (Figure 2c) represent larger lateral forces between tip (silicon nitride) and substrate and can be assigned to DPPS-enriched domains. In general, contrast in lateral force images originates from differences in adhesion, elasticity differences causing variable contact areas, and the roughness of the sample.[25–27] Lateral forces also occur due to topographic features of the sample, which can be distinguished, however, from those resulting from friction by changing the scan

  1439-4227/01/02/07-08 $ 17.50+.50/0 CHEMBIOCHEM **2001**, No. 7/8

direction. While lateral forces originating from topography do not depend on the scan direction, contrast based on material differences is characterized by contrast inversion if the scanning direction is reversed. The observed contrast inversion in the forward (Figure 2c) and backward scan direction (Figure 2d) confirms that the observed lateral contrast originates from material differences. The higher friction on the DPPS-enriched domains is probably due to a Ca^{2+}-induced solidification of DPPS giving rise to a higher critical shear modulus. From area analysis we concluded that $(32 \pm 3)\%$ of the overall area in the LFM image is occupied by the circularly shaped DPPS-enriched domains, which corresponds well to the values obtained from TOF-SIMS imaging and protein domain coverage. Comparing the protein coverage of $(35 \pm 3)\%$ with that of the DPPS-enriched domains demonstrates that annexin I solely binds to the acidic phospholipid domains and does not interact with zwitterionic DPPC molecules. Calcium ions are essential for annexin I binding at pH 7.4 as demonstrated in the experiment depicted in Figure 3. Annexin I that is adsorbed to DPPS domains immediately desorbs from the surface upon addition of a buffer containing ethylene glycol-bis(β-aminoethyl ether)-*N*,*N*,*N*′,*N*′-tetraacetic acid (EGTA), which removes the calcium ions from the bulk phase by complexation. Since calcium ions bound to the convex side of annexin I act as bridges connecting the protein with anionic lipid headgroups, the protein is released upon removing Ca^{2+}. By means of TOF-SIMS imaging and lateral force microscopy it was demonstrated that the DPPS-enriched domains do not form in the presence of EGTA.[24] However, as protein desorption occurs within minutes, we rule out that the DPPS-enriched domains have been dispersed within this time period, and cause protein desorption. Binding and desorption of the protein to the DDPS-enriched domains is fully reversible. However, annexin I molecules that are bound to defects in the lipid bilayer (small bright dots) remain adsorbed after the addition of an EGTA-containing buffer probably due to a preferentially hydrophobic interaction between the proteins and lipids at the edges.

We conclude that annexin I specifically binds to the interface of DPPS-enriched domains in a monomolecular fashion. Moreover, annexin I is capable of aggregating in the membrane-bound state and calcium ions are essential for protein binding at pH 7.4. It remains to be elucidated whether the role of calcium ions lies in membrane organization, that is domain formation, and if these domains are required for binding of the protein to the phosphatidylserine headgroups.

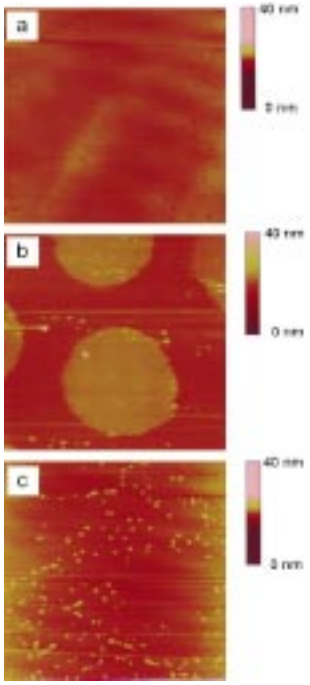

Figure 3. *Topographic images of a DPPC – DPPC/DPPS Langmuir – Blodgett bilayer deposited on mica obtained in 50 mM Tris (pH 7.4), 1 mM $CaCl_2$ before (a) and after addition of 1 μM annexin I (b). c: Scanning force microscopy image after rinsing the surface with 50 mM Tris (pH 7.4), 5 mM EGTA. All images are $10 \times 10\ \mu m^2$ in size.*

Experimental Section

Materials: DPPC and DPPS were purchased from Avanti Polar Lipids (Alabaster, AL, USA) and used without further purification. Recombinant porcine annexin I was purified according to Rosengarth et al.[28] Protein concentration was determined by UV absorption with $\varepsilon_{280} = 0.6\ cm^2\ mg^{-1}$. Protein purity was analyzed by SDS-PAGE.

Langmuir – Blodgett (LB) mono- and bilayer preparation: LB films were prepared on a Wilhelmy film balance equipped with a 25-mL teflon trough (15.4 cm × 2.5 cm) and a dipper device. For TOF-SIMS measurements LB films were deposited on precleaned gold-covered glass slides. Lipid films compressed at a rate of $1.8\ cm^2\ min^{-1}$ to a surface pressure of $30\ mN\ m^{-1}$ were transferred with a speed of $0.7\ mm\ min^{-1}$ while maintaining the surface pressure at $30\ mN\ m^{-1}$. LB films for SFM measurements were deposited on freshly cleaned mica plates dipped into a pure water subphase. First, a DPPC monolayer compressed to a surface pressure of $45\ mN\ m^{-1}$ was transferred onto mica followed by the deposition of a second monolayer composed of DPPC/DPPS (4:1) at $30\ mN\ m^{-1}$.[24]

Time-of-flight secondary-ion mass spectrometry (TOF-SIMS): The device and measurement procedure has been described elsewhere.[22, 23] Lateral resolution of 0.5 – 1 μm was obtained, corresponding to scan areas of $30 \times 30\ \mu m^2$ in a 256 × 256-raster. A mass spectrum (solely positive ions) was obtained by integrating SI intensities over the entire scan area.

Scanning force microscopy (SFM): Surface images of solid-supported membranes were obtained in an open fluid chamber using a Nanoscope IIIa Bioscope scanning force microscope (Digital Instruments, Santa Barbara, CA) operating in contact mode, equipped with a $100 \times 100\text{-}\mu m^2$ G scanner. For topography and lateral force microscopy images, microfabricated silicon nitride tips (NP-S, Digital Instruments) with an approximate tip radius of 5 – 20 nm and a spring constant of 0.06 – 0.1 $N\ m^{-1}$ were used as purchased. Minimal load force (200 – 400 pN) was employed during contact mode imaging, while the scan rate was set as high as possible (4 – 7 Hz for a $20 \times 20\text{-}\mu m^2$ image) to reduce the extent of bilayer deformation. For lateral force images higher load forces were applied.

C.S. thanks the state Nordrhein-Westfalen for a Lise Meitner habilitation fellowship and A.J. the DFG for a habilitation fellowship (JA 963 1/1). The authors are very much indebted to R. Kamischke and Prof. A. Bennighoven for providing the TOF-SIMS images and to Prof. H.-J. Galla for his support.

[1] V. Gerke, S. E. Moss, *Biochim. Biophys. Acta* **1997**, *1357*, 129 – 154.
[2] J. Mollenhauer, *Cell Mol. Life Sci.* **1997**, *53*, 506 – 507.
[3] S. Liemann, R. Huber, *Cell Mol. Life Sci.* **1997**, *53*, 516 – 521.
[4] A. Rosengarth, V. Gerke, H. Luecke, *J. Mol. Biol.* **2001**, *306*, 489 – 498.
[5] J. Benz, A. Hofmann, *Biol. Chem.* **1997**, *378*, 177 – 183.
[6] R. Huber, J. Römisch, E. P. Paques, *EMBO J.* **1990**, *9*, 3867 – 3874.
[7] D. Voges, R. Berendes, A. Burger, P. Demange, W. Baumeister, R. Huber, *J. Mol. Biol.* **1994**, *238*, 199 – 213.
[8] M. A. Swairjo, N. O. Concha, M. A. Kaetzel, J. R. Deman, B. A. Seaton, *Nat. Struct. Biol.* **1995**, *2*, 968 – 974.
[9] E. Bitto, W. Cho, *Biochemistry* **1998**, *37*, 10231 – 10237.
[10] E. Bitto, W. Cho, *Biochemistry* **1999**, *38*, 14094 – 14100.
[11] M. Jost, K. Weber, V. Gerke, *Biochem. J.* **1994**, *298*, 923 – 930.
[12] M. Jost, C. Thiel, K. Weber, V. Gerke, *Eur. J. Biochem.* **1992**, *207*, 923 – 930.
[13] M. R. Nelson, C. E. Creutz, *Biochemistry* **1995**, *34*, 3121 – 3132.
[14] M. de la Fuente, V. Parra, *Biochemistry* **1995**, *34*, 10393 – 10399.
[15] L. Oshry, P. Meers, T. Mealy, A. I. Tauber, *Biochim. Biophys. Acta* **1991**, *1066*, 239 – 244.
[16] W. Wang, C. E. Creutz, *Biochemistry* **1994**, *33*, 275 – 282.
[17] X. Weng, H. Luecke, I. S. Song, D. S. Kang, S. H. Kim, R. Huber, *Protein Sci.* **1993**, *2*, 448 – 458.
[18] E. Bitto, M. Li, A. M. Tikhonov, M. L. Schlossman, W. Cho, *Biochemistry* **2000**, *39*, 13469 – 13477.
[19] I. Reviakine, W. Bergsma-Schutter, A. Brisson, *J. Struct. Biol.* **1998**, *121*, 356 – 361.
[20] I. Reviakine, A. Simon, A. Brisson, *Langmuir* **2000**, *16*, 1473 – 1477.
[21] I. Reviakine, W. Bergsma-Schutter, C. Mazeres-Dubut, N. Govorukhina, A. Brisson, *J. Struct. Biol* **2000**, *131*, 234 – 239.
[22] N. Bourdos, F. Kollmer, A. Benninghoven, M. Ross, M. Sieber, H.-J. Galla, *Biophys. J.* **2000**, *79*, 357 – 369.
[23] N. Bourdos, F. Kollmer, A. Benninghoven, M. Sieber, H.-J. Galla, *Langmuir* **2000**, *16*, 1481 – 1484.
[24] M. Ross, C. Steinem, H.-J. Galla, A. Janshoff, *Langmuir* **2001**, *17*, 2437 – 2445.
[25] J. N. Israelachvilli in *Fundamentals of Friction: Macroscopic and Microscopic Processes* (Ed.: I. L. Singer, H. M. Pollock), Kluwer, Dordrecht, The Netherlands, **1992**, pp. 351 – 385.
[26] S. Grafström, J. Ackermann, T. Hagen, R. Neumann, O. Probst, *J. Vac. Sci. Technol. B* **1994**, *12*, 1559 – 1564.
[27] S. Grafström, M. Neitzert, T. Hagen, J. Ackermann, R. Neumann, O. Probst, M. Wörtge, *Nanotechnology* **1993**, *4*, 143 – 151.
[28] A. Rosengarth, J. Rösgen, H.-J. Hinz, V. Gerke, *J. Mol. Biol.* **1999**, *288*, 1013 – 1025.

Received: February 5, 2001 [Z190]

Electroactive Monolayer Substrates that Selectively Release Adherent Cells

Woon-Seok Yeo, Christian D. Hodneland, and Milan Mrksich*[a]

KEYWORDS:

biosurfaces · cell adhesion · dynamic substrates · electrochemistry · monolayers

This communication describes a dynamic substrate that can selectively release immobilized ligands and hence can regulate, in real-time, the ligand – receptor interactions between a cell and the substrate to which it is attached. The aim of this work is to provide model substrates for mechanistic studies of cell adhesion and migration. The adhesion of cells is mediated by the binding of cell-surface receptors—often, the integrin family of receptors—to ligands of the insoluble protein matrix (also known as the extracellular matrix).[1] In many cases, cells respond to changes in the composition of ligands presented within the matrix. Examples are found in the growth or differentiation of cells,[2] and in tumor metastasis, where malignant cells migrate through the endothelial barrier.[3] The development of dynamic substrates which can modulate the composition of ligands that interact with adherent cells would provide new opportunities for studying many important cellular processes. In this paper, we describe a chemical strategy to develop a dynamic substrate that can selectively release immobilized ligands under electrochemical control.

Our approach is based on a self-assembled monolayer (SAM) of alkanethiolates on gold that presents peptide ligands tethered to the monolayer through an electroactive quinone ester moiety (Scheme 1 B). The quinone ester undergoes a two-electron reduction on application of an electrical potential to the underlying gold substrate to give the corresponding hydroquinone, which then rapidly cyclizes to give a lactone with release of the peptide ligand.[4, 5] We use as a model system, a monolayer that can release the tripeptide Arg-Gly-Asp (RGD). This peptide is a ligand found within many extracellular matrix proteins and which mediates cell adhesion through integrin receptors.[1] With this system, the application of an electrical potential results in the release of RGD and, therefore, of cells that are attached to the monolayer. This model system has the benefits that the dynamic property can be easily visualized, and that it establishes the compatibility of the electroactive substrate with the conditions of cell culture. The tri(ethylene glycol)

[a] *Prof. Dr. M. Mrksich, W.-S. Yeo, Dr. C. D. Hodneland*
Department of Chemistry
University of Chicago
5735 South Ellis Avenue
Chicago, IL 60637 (USA)
Fax: (+1) 773-702-0805
E-mail: mmrksich@midway.uchicago.edu

